RESEARCH PAPERS

Acta Cryst. (1997). D**53**, 231–239

Partial Improvement of Crystal Quality for Microgravity-Grown Apocrustacyanin C_1

E. H. SNELL,[a]† A. CASSETTA,[a]‡ J. R. HELLIWELL,[a]* T. J. BOGGON,[a] N. E. CHAYEN,[b] E. WECKERT,[c] K. HÖLZER,[c] K. SCHROER,[c] E. J. GORDON[d] AND P. F. ZAGALSKY[e]

[a]*Chemistry Department, University of Manchester M13 9PL, England,* [b]*Biophysics Section, The Blackett Laboratory, Imperial College of Science, Technology and Medicine, London SW7 2BZ, England,* [c]*Institut für Kristallographie, University of Karlsruhe (TH), Kaiserstrasse 12, Postfach, 6980 D-76128 Karlsruhe, Germany,* [d]*Institut de Biologie Structurale, Laboratoire de Cristallographie Macromoleculaire, 41 avenue des Martyrs-38027, Grenoble CEDEX, France, and* [e]*Biochemistry Department, Royal Holloway, University of London, Egham, Surrey TW20 0EX, England.*
E-mail: john.helliwell@man.ac.uk

(*Received 1 May 1996; accepted 8 November 1996*)

Abstract

The protein apocrustacyanin C_1 has been crystallized by vapour diffusion in both microgravity (the NASA space shuttle USML-2 mission) and on the ground. Rocking width measurements were made on the crystals at the ESRF Swiss–Norwegian beamline using a high-resolution ψ-circle diffractometer from the University of Karlsruhe. Crystal perfection was then evaluated, from comparison of the reflection rocking curves from a total of five crystals (three grown in microgravity and two earth controls), and by plotting mosaicity *versus* reflection signal/noise. Comparison was then made with previous measurements of almost 'perfect' lysozyme crystals grown aboard IML-2 and Spacehab-1 and reported by Snell *et al.* [Snell, Weisgerber, Helliwell, Weckert, Hölzer & Schroer (1995). *Acta Cryst.* D**51**, 1099–1102]. Overall, the best diffraction-quality apocrustacyanin C_1 crystal was microgravity grown, but one earth-grown crystal was as good as one of the other microgravity-grown crystals. The remaining two crystals (one from microgravity and one from earth) were poorer than the other three and of fairly equal quality. Crystal movement during growth in microgravity, resulting from the use of vapour-diffusion geometry, may be the cause of not realising the 'theoretical' limit of perfect protein crystal quality.

1. Introduction

Microgravity has been used as a crystallization environment for improving protein crystal quality through reduced sedimentation and convection effects. Growth in microgravity has been shown to reduce the mosaicity of lysozyme crystals with a resulting increase in the signal-to-noise ratio of reflection intensity data, thereby facilitating measurement of weaker high-resolution data (Snell *et al.*, 1995; Helliwell, Snell & Weisgerber, 1995). The mosaic spread, unlike resolution limit, is a crystal parameter which can be independent of the incident X-ray beam and detector setup, and gives a direct indication of the geometric perfection of a crystal. It does however, require a finely collimated beam and high-resolution diffractometer to avoid the beam effects smearing out the rocking width so as to analyse the reflection in detail (Helliwell, 1988).

In the event of a reduction in mosaicity in the crystal this should manifest in an enhancement of the signal-to-noise ratio of the reflection intensity measured, provided extinction is absent, and is particularly valuable for considering the optimization of the measurement of weak high-resolution protein diffraction data. In our previous report (Snell *et al.*, 1995) this was strongly manifest in favour of microgravity-grown crystals of lysozyme over earth-grown controls on two separate missions measured by two different methods. Moreover, the microgravity-grown crystals were the most perfect protein crystals ever reported to date, very close to the theoretical limit, and thereby setting bounds on the size of diffraction apparatus that might usefully be considered (*e.g.* several metres for the crystal-to-detector distance, which in turn defines a maximum useful detector size for a given X-ray wavelength). In Snell *et al.* (1995) it was readily possible to find reflections at 1.2 Å by use of a 0.0002° angular step scan, with an instrument resolution function of 0.00195° on the ESRF Swiss–Norwegian bending magnet beamline. In contrast, with a 1° scan, Vaney, Maignan, Riès-Kautt & Ducriux (1996) at the LURE synchrotron obtained a resolution limit of 1.4 Å for a microgravity-grown lysozyme crystal.

The purpose of this paper is to extend the comparisons of protein crystal quality to other protein cases. We report here the mosaicity measurements on apocrustacyanin C_1.

† Current address: NASA Laboratory for Structural Biology, Code ES76, Building 4464, Marshall Space Flight Center, Huntsville, Al 35812, USA.

‡ EU Fellow, on leave from CNR, Istituto di Strutturistica Chimica Sez. Trieste, Padriciano 99, Trieste, Italy.

ISSN 0907-4449

2. Experimental

2.1. *Crystallization*

The crystallization of the protein apocrustacyanin C_1, a subunit of the α-crustacyanin protein responsible for the blue colouration of the carapace of the lobster *Homarus gammorus* has been described elsewhere (Chayen, Gordon & Zagalsky, 1996). Apocrustacyanin C_1, molecular weight 20 kDa, crystallizes in space group $P2_12_12_1$, $a = 42.1$, $b = 81.0$, $c = 110.7$ Å and $\alpha = \beta = \gamma = 90°$ with two subunits per asymmetric unit. For the experiment reported here the protein solution (20 mg ml^{-1} in 0.1 *M* Tris–HCl, 1 m*M* EDTA pH 7.0) was mixed 1/1(*v*/*v*) with a reservoir solution [5%(*v*/*v*) 2-methyl-2,4-pentanediol (MPD), 1 m*M* EDTA, 0.1 *M* Tris–HCl pH 9.0 and 1.9 *M* ammonium sulfate] to form 50 µl drops.

The microgravity equipment for crystallization was the European Space Agency (ESA) Advanced Protein Crystallization Facility (APCF) (Snyder, Fuhrmann & Walter, 1991; Bosch, Lautenschlager, Potthast & Stapelmann, 1992). The APCF is a modular system containing 48 reactors each allowing one of three modes of crystallization namely, dialysis, liquid–liquid (free interface) and vapour diffusion. The vapour-diffusion reactor used in this case consists of a reservoir formed by two porous, ultra high molecular weight, polythene blocks (each holding 0.35 ml of solution) and protein solution held in a glass cylindrical tube which can be raised to activate crystallization. The APCF was flown

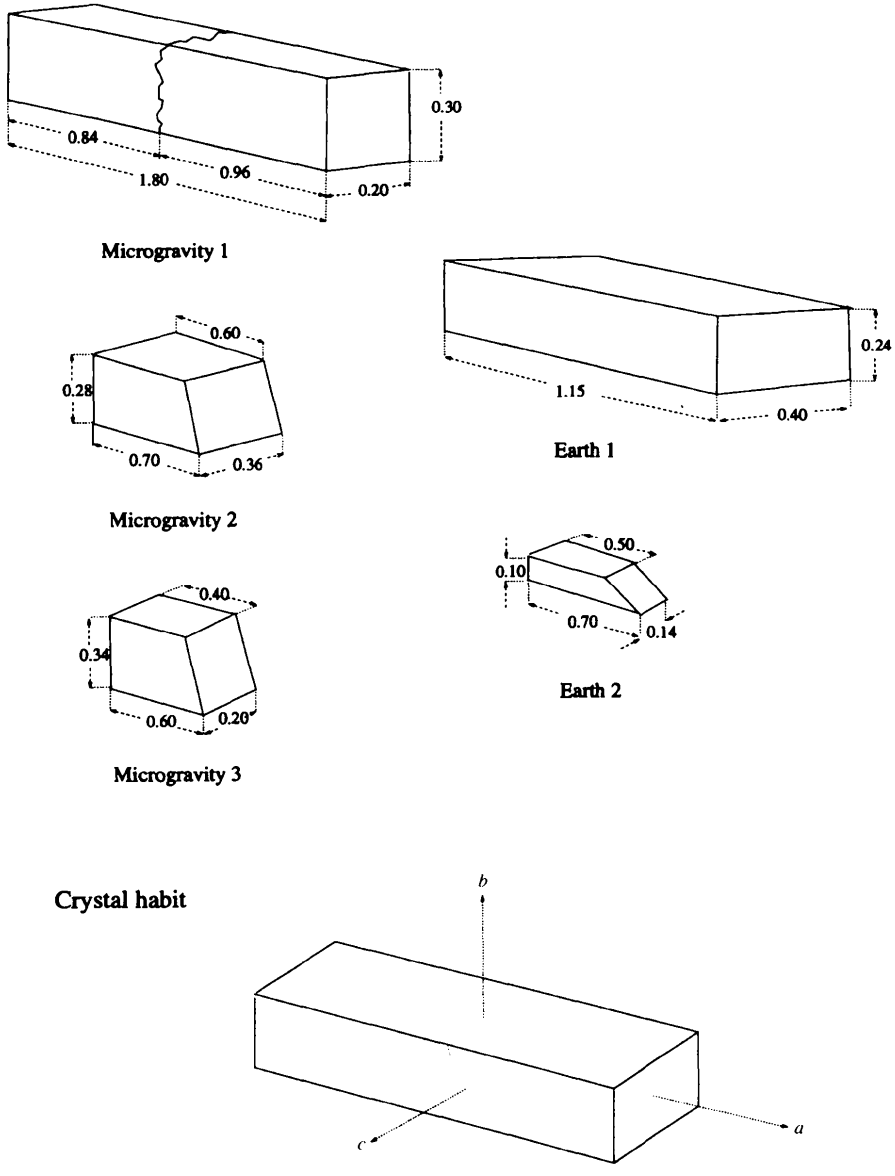

Fig. 1. Dimensions of apocrustacyanin C_1 crystals used for data collection (not to scale). The relationship of the crystal habit and the unit-cell parameters is also shown.

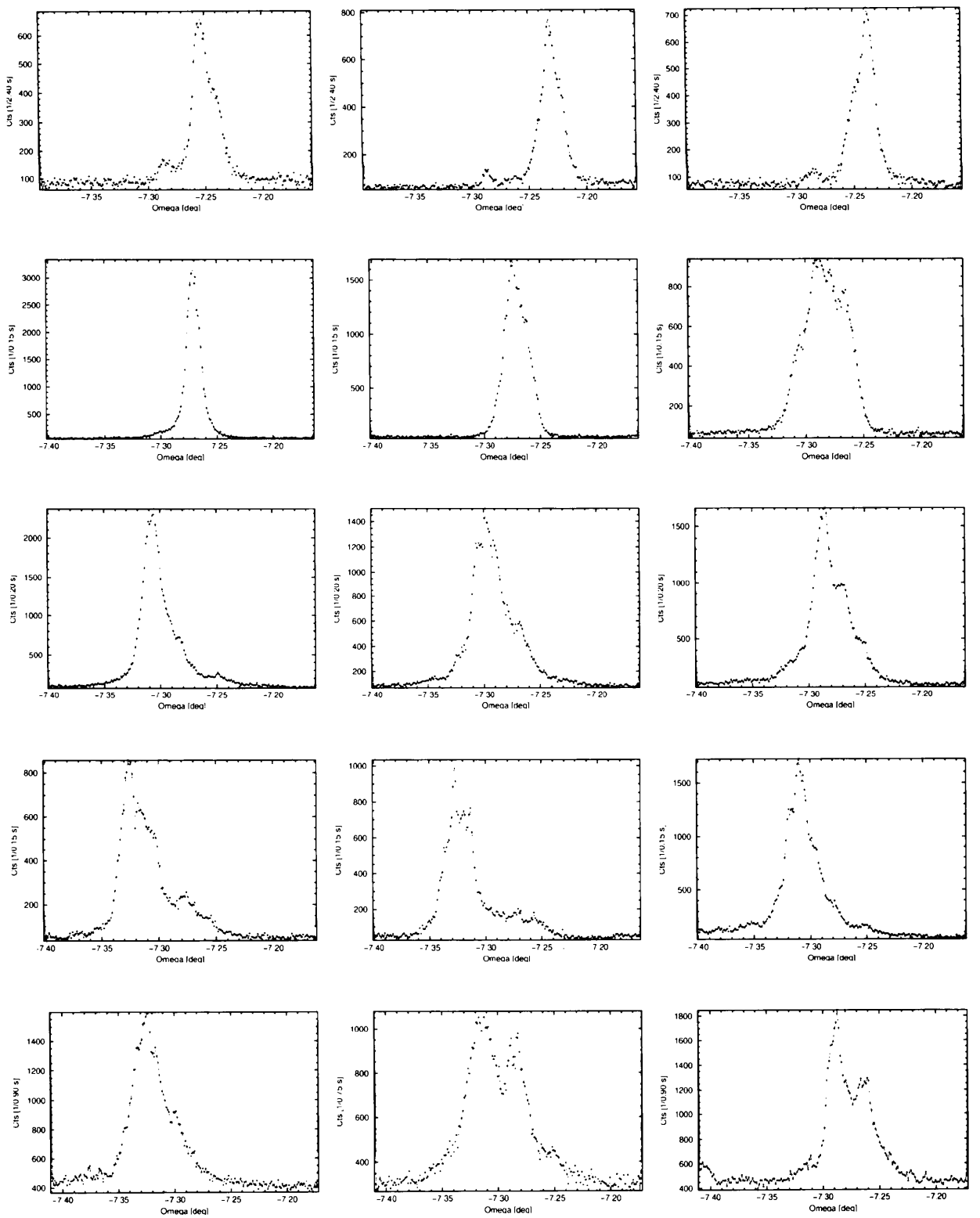

Fig. 2. Rocking curves for the (4 19 1) reflection (4 Å resolution), as a representative example, at three ω settings (left to right), for each of the five crystals, μg 1 (first row), μg 2 (second row), μg 3 (third row), earth 1 (fourth row) and earth 2 (fifth row). The three curves for μg 1 (first row) were measured in single-bunch mode, *i.e.* where the circulating current is approximately 1/10th of the current available for all the other curves.

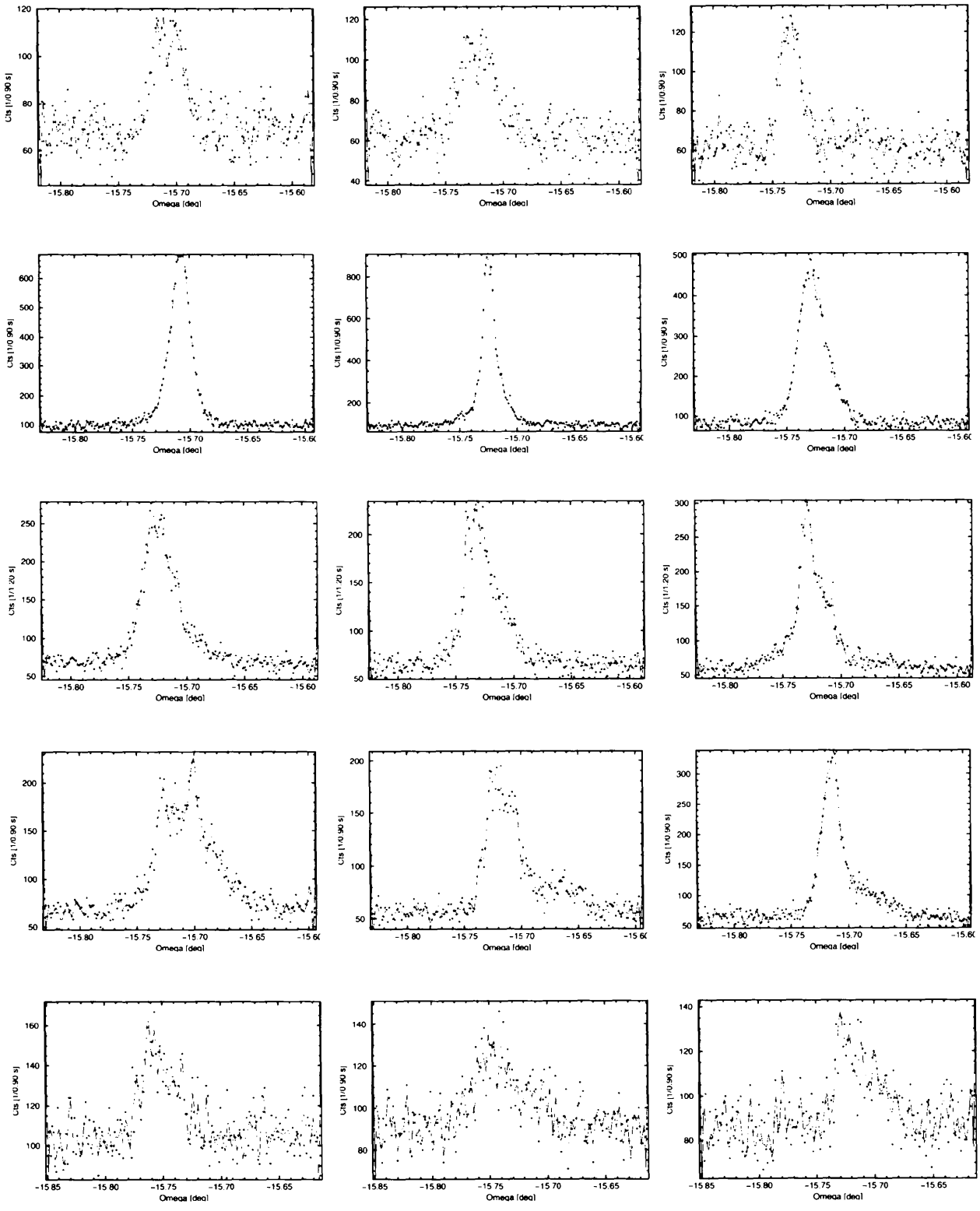

Fig. 3. Rocking curves for the (11 22 43) reflection (1.85 Å resolution), as a representative example, laid out in the same format as in Fig. 2. This reflection, being at high resolution, was measured near the start of the run for each crystal [unlike the (4 19 1) reflection which was measured near the end of the sequence of reflections, being at low resolution]. This essentially avoids any impact of radiation damage.

on board the United States Microgravity Laboratory-2 (USML-2), STS-73, NASA space shuttle mission. Crystallization took place over a period of 14 d 11 h 17 min (347 h 17 min) of microgravity time at a temperature of 273 ±0.1 K. Ground controls were grown simultaneously with identical materials in identical apparatus with temperature control also to ±0.1 K.

2.2. *Data collection*

Measurement of the rocking widths by monochromatic methods requires a synchrotron X-ray beam with very low divergence and small $\delta\lambda/\lambda$. This has to be combined with a small angular step size diffractometer to fully probe the rocking width in detail. Data collection took place on station A of the joint Swiss–Norwegian beamline at the ESRF. The Swiss–Norwegian beamline has a Huber ψ-circle diffractometer. The primary role of this diffractometer is the direct determination of triplet phases (Hümmer, Weckert & Bondza, 1989; Weckert, Schwegle & Hümmer, 1993). The instrument contains two circles (θ, ν) for the detector with axes perpendicular to each other and four circles for the crystal motion. The first crystal axis is parallel to the first detector axis (ω–2θ relation). Perpendicular to the ω -axis a second axis for the ψ rotation is installed. This ψ-axis bears an Eulerian cradle with motions χ and φ. Thus, an arbitrary scattering vector **h** can be aligned with the ψ-axis and a ψ-scan *(i.e.* rotation around a reciprocal lattice vector for any *hkl*) performed by moving only one circle (with a consequent improvement in accuracy).

A total of three microgravity-grown crystals and two earth-grown crystals (Fig. 1) were mounted in glass capillaries of 1.0 mm diameter for data collection. The three microgravity crystals were of approximate volume 0.108, 0.06 and 0.03 mm^3 (labelled μg 1, 2 and 3, respectively). No artificial mother liquor was used but plugs of stabilizing solution (2.0 *M* ammonium sulfate) were placed at either end of the capillaries before sealing with wax. Unfortunately, the largest microgravity crystal, μg 1, showed a crack across it half way down its length. The two ground control crystals were of approximate volume 0.11 and 0.01 mm^3 (labelled earth 1 and 2, respectively) and were also mounted in 1.0 mm glass capillaries. For each crystal the same set of 60 different reflections (over a resolution range of 12.39–1.44 Å) were measured at three ψ angles of –45, 0 and 45°. There was no appreciable difference in the incident intensity between the start and end of the reflection scans. Fig. 2 shows, as examples, the rocking curves for the (4 19 1) reflection for three ψ settings for each of the five crystals and, likewise, Fig. 3 shows the curves for the (11 22 43) reflection.

The instrument resolution function (IRF′) (Colapietro *et al.*, 1992) was calculated at 0.00195° excluding the

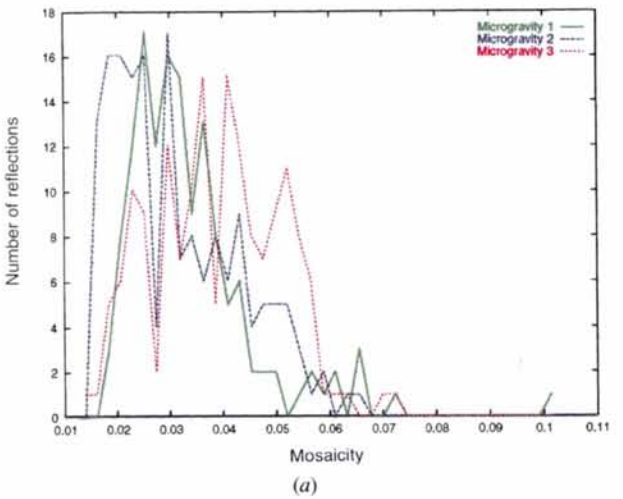

(*a*)

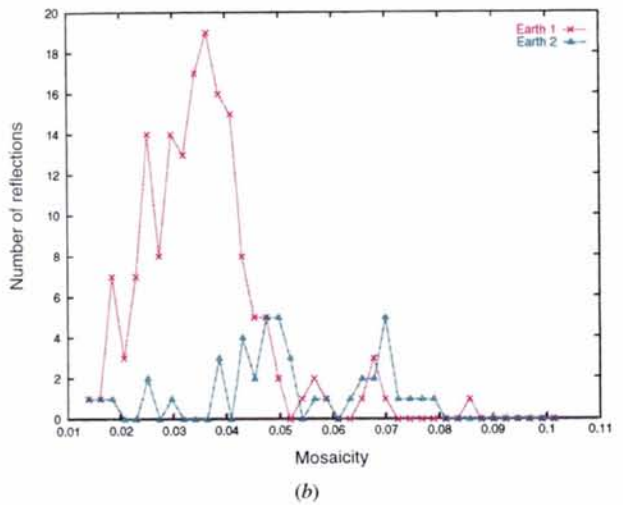

(*b*)

Fig. 4. Histogram of the mosaicity for (*a*) the three microgravity and (*b*) two earth-grown apocrustacyanin C_1 crystals.

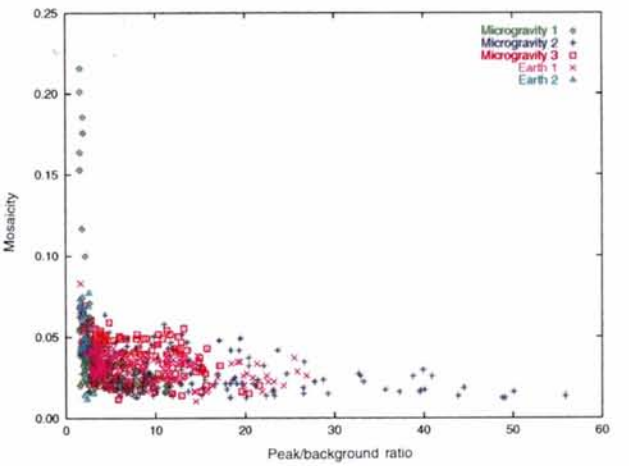

Fig. 5. Plot of the mosaicity *versus* peak/background for the three microgravity-grown and two earth-grown control crystals of apocrustacyanin C_1.

reflection-dependent $(\Delta\lambda/\lambda)\tan\theta$ component, which was dealt with on a per reflection basis (*i.e.* according to the appropriate θ angle). The source-to-instrument distance was 45 m with a double crystal Si(111) monochromator providing a 1 Å wavelength beam. The vertical beam source size was, at full width at half maximum (FWHM), 200 μm and the wavelength bandpass, $\delta\lambda/\lambda$, equal to 2×10^{-4}.

2.3. *Data processing*

The boundary of the reflection was determined by the Lehmann–Larsen (Lehmann & Larsen, 1974) method. This allows determination of the reflection background boundary as a minimum in $\sigma(I)/I$ over the range of each reflection profile. This was used because some of the reflections were quite weak. The scattering angle, θ, was then evaluated and also the FWHM, φ_R, of the reflection measured. The crystal sample mosaicity, η, can be determined by deconvoluting out these geometric and spectral parameters from the measured φ_R by use of,

$$\eta = (\varphi_R^2 - \mathrm{IRF}'^2)^{1/2},$$

where IRF′ is the reflection-dependent instrument resolution function (Colapietro *et al.*, 1992)

3. Results and discussion

Table 1 illustrates the maximum, minimum and standard deviation of the mosaicity values obtained from the crystals. Crystal μ*g* 1, which displayed a crack (as referred to above), displayed the second highest average mosaicity as well as the worst maximum and minimum values. Because of the crack this crystal, unfortunately, has to be discounted for the purposes of comparison (other than its volume). None of the minimum values reach the quality of the lysozyme mosaicity results obtained previously (Snell *et al.*, 1995). On the basis of the number of unit cells in each direction of the crystal habit (and the respective unit-cell size in each direction) we can calculate minimum mosaicity values (Helliwell, 1988), *e.g.* for earth 1, of $0.00021 \times 0.0019 \times 0.0016°$. Hence, the theoretical limit isn't approached either. On the basis of Table 1 there is no clear distinction in favour of microgravity *versus* earth grown crystals, μ*g* 2 being marginally the best $\langle\eta\rangle$ and with the lowest maximum η but earth 1 and μ*g* 3 have the best minimum η. A population analysis of the mosaicity values for the crystals is shown in Fig. 4. If any discrimination is to be found between the crystals grown by the two different routes then we need a more sensitive measurement

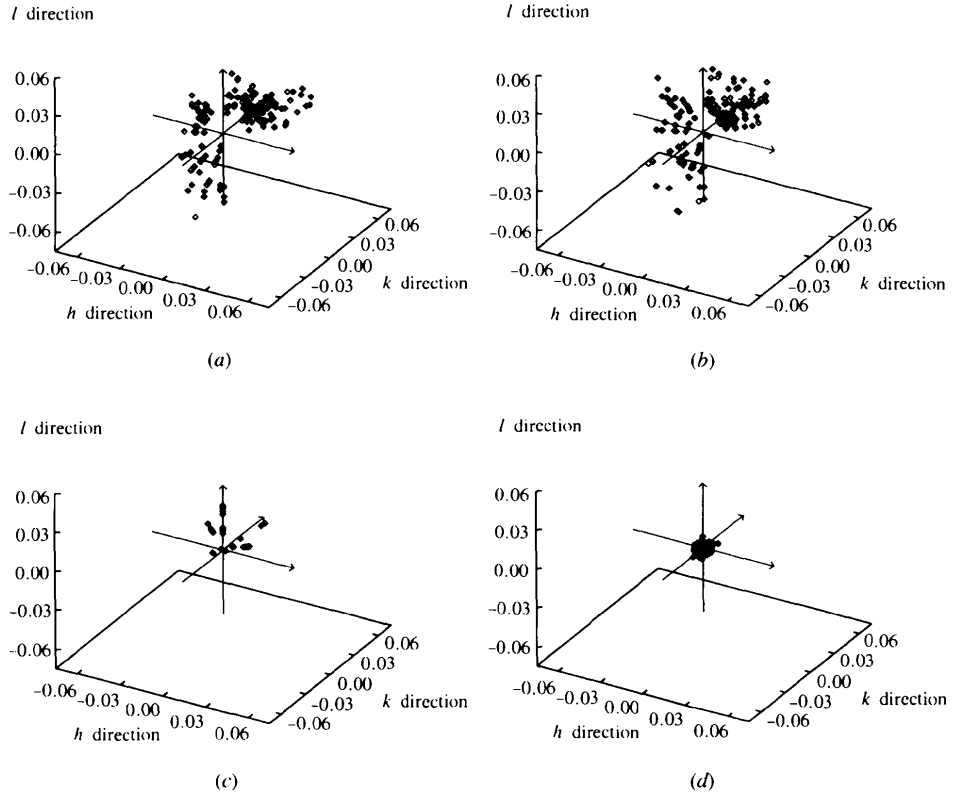

Fig. 6. Plot of the 'mosaicity (rocking) volume' for (*a*) earth 1 apocrustacyanin, (*b*) μ*g* 3 apocrustacyanin, (*c*) earth-grown lysozyme and (*d*) microgravity-grown lysozyme [Snell *et al.* (1995) for (*c*) and (*d*)]. All plots are on the same scale with the mosaicities given in °.

Table 1. *Analysis of η values (°) for the apocrustacyanin C_1 crystals measured*

Crystal	Max η	Min η	$\langle\eta\rangle$	$\sigma(\eta)$	Reflections
μg 1	0.2160	0.0167	0.0393	0.0328	148
μg 2	0.0648	0.0143	0.0303	0.0118	168
μg 3	0.0708	0.0131	0.0378	0.0118	164
Earth 1	0.0840	0.0118	0.0344	0.0110	165
Earth 2	0.0780	0.0131	0.0501	0.0164	44

than the mosaicity provides in this case. Towards that end, a plot of mosaicity *versus* peak/background, was investigated and is shown in Fig. 5. It can be seen clearly (also in the raw data in Figs. 2 and 3) that μg 2 produces much higher peak-to-background ratio (*i.e.* better signal-to-noise ratio) than the other crystals for the same set of reflections. One other μg crystal and an earth crystal are of comparable, very good, quality (μg 3 and earth 1). The poorest quality crystals are μg 1 and earth 2, the former's low quality was probably a result of crystal splitting. The poor quality of μg 1 and earth 2 is clearly seen in Fig. 3, the high-resolution reflection (11 22 43), is well measured for μg 2, μg 3 and earth 1 only.

A large range of values within the crystals we suspect strongly suggests, Table 2, an anisotropic mosaicity for the crystals. To investigate the possible anisotropy in the mosaicity a 'mosaicity volume' plot can be made, *i.e.* plotting the unit diffraction vector of a reflection along with its magnitude as the mosaicity (a mosaicity vector). Figs. 6(*a*) and 6(*b*) show this for the apocrustacyanin (earth-grown and microgravity-grown reflections, respectively) and Figs. 6(*c*) and 6(*d*), for comparison, show values from our previous work with lysozyme (earth-grown and microgravity-grown, IML-2 mission, respectively) (Snell *et al.*, 1995) using the same scale. This demonstrates pictorially the level of improvement that can be made towards producing perfect crystals (in the ideal case of an infinitely large perfect crystal the rocking volume would be a point). Fig. 7 illustrates the

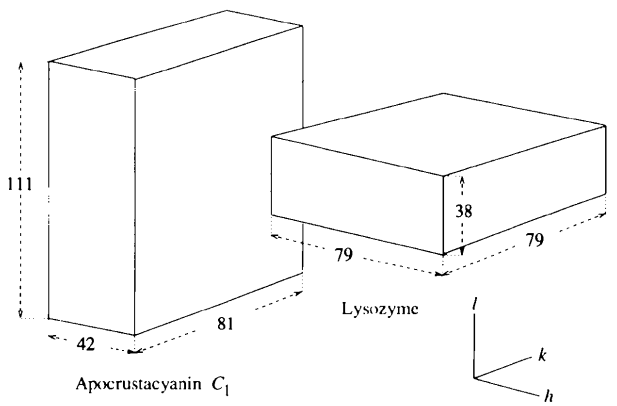

Fig. 7. Unit-cell dimensions of apocrustacyanin C_1 and lysozyme (in Å).

Table 2. *Mosaicity volume ellipsoid parameters for both apocrustacyanin C_1 and lysozyme crystals*

The parameters η_x, η_y and η_z being the maximum mosaicity vector, in the x, y and z directions, respectively (values in °).

Crystal	η_x	η_y	η_z	η volume
μg 1	0.1624	0.1777	0.1446	0.01748
μg 2	0.0298	0.0641	0.0459	0.00037
μg 3	0.0364	0.0496	0.0592	0.00045
Earth 1	0.0397	0.0681	0.0754	0.00085
Earth 2	0.0258	0.0743	0.0543	0.00044
Earth lysozyme	0.0254	0.0254	0.0341	0.00009
μg lysozyme	0.0069	0.0100	0.0069	0.000002

relative dimensions of the unit cells in the same orientation of the mosaicity volume plot with Fig. 1 showing the crystal habit of apocrustacyanin C_1. Fig. 8 shows the two-dimensional projection of the 'mosaicity volume' onto the *hk* and *hl* planes. The 'mosaicity volume' is evaluated as the volume of an ellipsoid having values of principal half axes as maximum mosaicity magnitude in x, y and z real-space directions (for space group $P2_12_12_1$, coaxial with h, k and l directions). Table 2 gives these ellipsoid parameters for the apocrustacyanin C_1 and comparison values for lysozyme. In the case of apocrustacyanin C_1 the consistently smallest mosaicity occurs along the h axis, correlated with the theoretical mosaicity along a. This is demonstrated in Table 2 with the exception of the cracked μg 1 crystal. With lysozyme, by comparison, the mosaicity is isotropic.

4. Concluding remarks

The plot of mosaicity *versus* signal/noise is very sensitive to crystal quality. In the case of apocrustacyanin the main noticeable improvement in crystal quality through microgravity growth is indeed as measured by this plot and manifest really only for one crystal. This is in contrast to the clear improvement for all the lysozyme crystals in our previous study (Snell *et al.*, 1995). How can this be explained? CCD observation of the vapour-diffusion crystallization of apocrustacyanin C_1 in microgravity has shown a rapid motion of crystals within the drop (Chayen, Snell, Helliwell & Zagalsky, 1997). CCD observation of other microgravity crystallizations based on different methods *e.g.* dialysis crystallization of lysozyme (Snell, Boggon, Helliwell, Moskowitz & Nadarajah, 1997) and free interface crystallization of α-crustacyanin onboard an unmanned space platform (Boggon, Chayen, Zagalsky, Snell & Helliwell, 1997) has shown a little and no motion, respectively. In the vapour-diffusion case for the apocrustacyanin C_1, this motion, probably resulting from Marangoni convection (Molenkamp, Janssen & Drenth, 1994; Savino & Monti, 1996), may well be the limiting factor on the quality of the crystals that can be produced. In comparison with

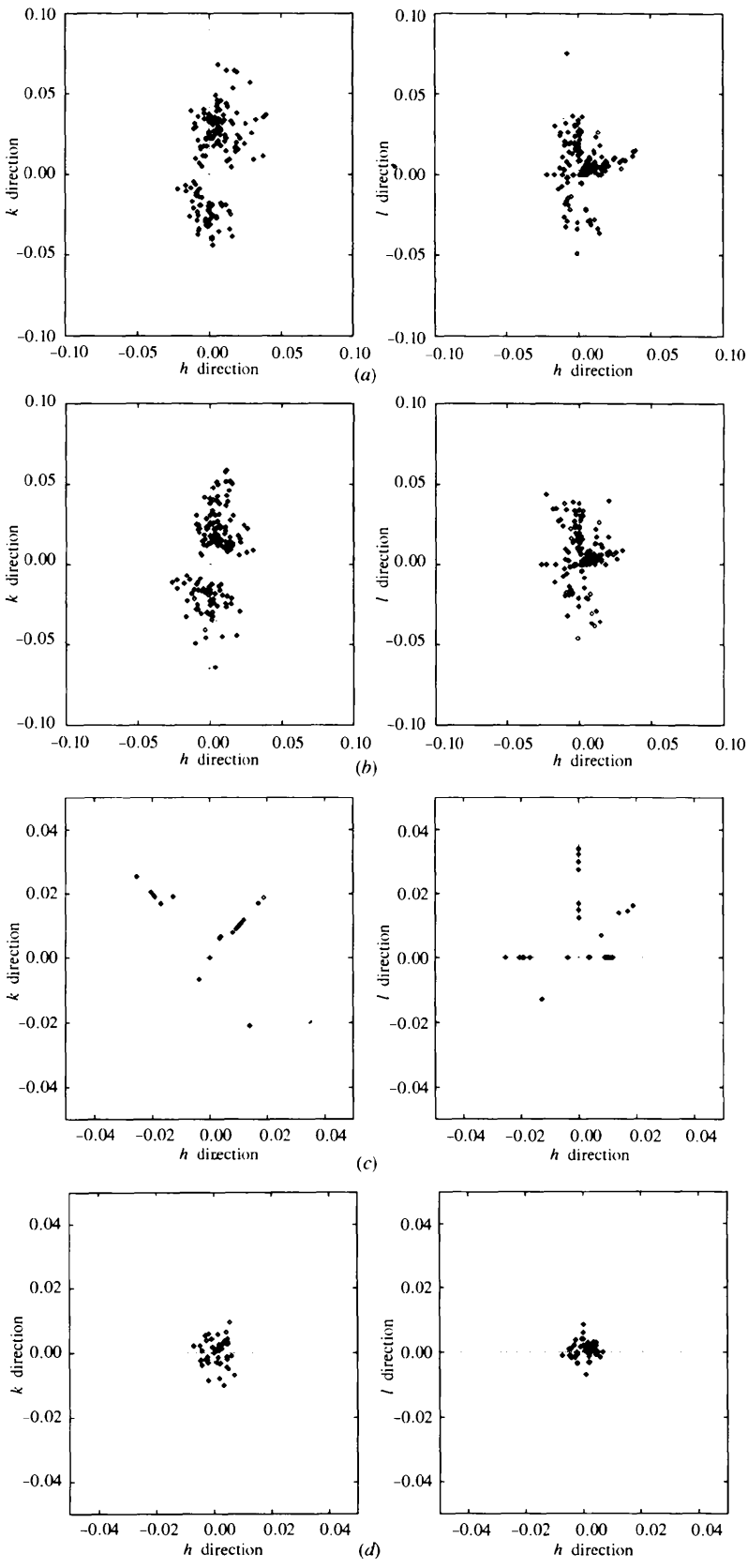

Fig. 8. Plot of the rocking volume projected onto the *hk* and *hl* planes for (*a*) earth 1 apocrustacyanin, (*b*) μ*g* 3 apocrustacyanin, (*c*) earth-grown lysozyme and (*d*) microgravity-grown lysozyme.

the microgravity-grown lysozyme crystal case there is room for improvement for the apocrustacyanin C_1, at least as evidenced by the mosaicity volume plots and the CCD video monitor. Hence, a repeat experiment of apocrustacyanin C_1 crystal growth in microgravity, but using dialysis or liquid–liquid diffusion (rather than vapour diffusion) suggests itself, whereby the crystals would remain stationary during the growth process. Moreover, with lysozyme, instead of dialysis (Helliwell *et al.*, 1995) vapour diffusion might be used, inducing crystal movement even in microgravity, so as to reduce the crystal perfection from that obtained previously (Snell *et al* ., 1995). Finally, in the Protein Crystallisation Diagnostic Facility (PCDF) being planned by ESA (Stapelmann *et al.*, unpublished work), a detailed history of a particular crystal growth process will be established *via* laser light scattering (nucleation step), interferometry (growth stage) and CCD video monitoring (to track crystal movement and growth), all prior to harvesting and full X-ray diffraction characterization and data collection for protein structure analysis.

We would like to express our thanks to the Swiss–Norwegian CRG at the ESRF, Grenoble for providing access to their beamline facilities and in particular to Dr Phil Pattison and his colleagues for their help. We are extremely grateful to ESA for flight opportunities and, in this particular study, for financing the beamtime at ESRF. Drs H. U. Walter, H. Martinides, K. Fuhrmann and O. Minster are thanked for their regular help and support. The Dornier and ESA staff are thanked for all their work in the development, support, and discussions with respect to APCF and PCDF apparatus. EHS and TJB are grateful to the EPSRC and the University of Manchester, respectively, for studentship support. PFZ acknowledges support from the EEC commission (grant ERBSCI-CI 920813). AC was an EU Host Institute Fellow in Manchester on leave from the CNR in Italy.

References

Boggon, T. J., Chayen, N. E., Zagalsky, P. F., Snell, E. H. & Helliwell, J. R. (1997). *Biophys. J.* Submitted.

Bosch, R., Lautenschlager, P., Potthast, L. & Stapelmann, J. (1992). *J. Cryst. Growth*, **122**, 310–316.

Chayen, N. E., Gordon, E. J. & Zagalsky, P. F. (1996). *Acta Cryst.* D**52**, 156–159.

Chayen, N. E., Snell, E. H., Helliwell, J. R. & Zagalsky, P. F. (1997). *J. Cryst. Growth*. In the press.

Colapietro, M., Cappuccio, G., Marciante, C., Pifferi, A., Spagna, R. & Helliwell, J. R. (1992). *J. Appl. Cryst.* **25**, 192–194.

Helliwell, J. R. (1988). *J. Cryst. Growth*, **90**, 259–272.

Helliwell, J. R., Snell, E. H. & Weisgerber, S. (1995). *Proceedings of 1995 Berlin Microgravity Conference*, edited by L. Ratke, H. Walter & B. Feuerbacher, pp. 155-170. Berlin: Springer-Verlag.

Hümmer, K., Weckert, E. & Bondza, H. (1989). *Acta Cryst.* A**45**, 182–187.

Lehmann, M. S. & Larsen, F. K. (1974). *Acta Cryst.* A**30**, 580–584.

Molenkamp, T., Janssen, L. P. B. M. & Drenth, J. (1994). *Final reports of sounding rockets in fluid science and material science, TEXUS 28 to 30, MAUSER 5 & MAXUS. ESA SP-1132*, Vol. 4, pp. 22–43.

Savino, R. & Monti, R. (1996). *J. Cryst. Growth*, **165**, 308–318.

Snell, E. H., Boggon, T. J., Helliwell, J. R., Moskowitz, M. E. & Nadarajah, A. (1997). *Acta Cryst.* D**53**. Submitted.

Snell, E. H., Weisgerber, S., Helliwell, J. R., Weckert, E., Hölzer, K. & Schroer, K. (1995). *Acta Cryst.* D**51**, 1099–1102.

Snyder, R. S., Fuhrmann, K. & Walter, H. U. (1991). *J. Cryst. Growth*, **110**, 333–338.

Vaney, M. C., Maignan, S., Riès-Kautt, M. & Ducriux, A. (1996). *Acta Cryst.* D**52**, 505–517.

Weckert, E., Schwegle, W. & Hümmer, K. (1993). *Proc. R. Soc. London Ser. A*, **442**, 33–46.